Int. J. Heat Mass Transfer. Vol. 35, No. 1, pp. 221–237, 1992
Printed in Great Britain

0017–9310/92 $5.00 + 0.00

Heat and mass transfer in a single screw extruder for non-Newtonian materials

S. GOPALAKRISHNA† and Y. JALURIA‡
Department of Mechanical and Aerospace Engineering, Rutgers University, New Brunswick, NJ 08903, U.S.A.

and

M. V. KARWE
Center for Advanced Food Technology, Rutgers University, New Brunswick, NJ 08903, U.S.A.

(*Received* 16 *January* 1990 *and in final form* 22 *January* 1991)

Abstract—Numerical simulation of the transport processes arising in a single screw extruder for non-Newtonian fluids such as plastics and food is considered. The study is directed mainly at simulating the heat and mass transfer inside the screw channel, for a power-law fluid. Moisture is taken as the species for mass transfer, since it is of particular interest in food processing. Finite difference computations are carried out to solve the governing set of partial differential equations for the velocity, temperature and moisture fields, over a wide range of governing parameters. The variation of viscosity with temperature and moisture is taken into account. The basic physical approach for modeling the complicated heat and mass transfer processes for inelastic non-Newtonian materials is outlined. As an application of this analysis to starch-based food systems, the reactive nature of the food constituents is incorporated by including the rate of reaction (gelatinization) between moisture and food. Results are presented in terms of the velocity, temperature and moisture concentration contours. Strong viscous dissipation effects are found to arise for typical operating conditions. The moisture contours indicate that starch gelatinization typically occurs first at the screw root. The effect of the various governing parameters on pressure build-up within the extruder channel is determined and discussed in terms of the underlying physical processes. Experimental validation of some of the numerical results has been carried out, and the comparisons are quite good. Results are also presented for the residence time distribution (RTD), an important design parameter in extrusion. Though this study considers moisture transport, the basic approach presented may easily be extended to reactions and mass transfer of other species in polymers and in other non-Newtonian materials.

1. INTRODUCTION

EXTRUSION is one of the most widely used manufacturing processes in industries dealing with materials such as rubber, plastics, polymers and pharmaceutical products. In screw extrusion, the raw material is fed into a hopper and is forced through the passage between a rotating screw and a stationary barrel. The processed material comes out through a die of a specific shape. Extrusion cooking has also become an important food processing operation in recent years. In this process, the raw food ingredients are subjected to a high shear and temperature environment. This results in mixing and leads to chemical reactions that constitute the cooking process. Single and twin screw extruders have been used extensively in the food industry. The relative merits of these two types of extruders and the state of the art have been reviewed recently [1]. Several experimental and numerical studies have been carried out to understand the physical phenomena involved in the thermal processing of polymeric materials in extrusion [2–4]. However, many areas are still in need of detailed further investigation, simulation and optimization.

Typically, a single screw extruder can be divided into three sections, as shown in Fig. 1. (1) The feed section, which is the region near the hopper; this section has a deep screw channel where the solid material is compacted and conveyed to the next section. (2) The compression section, where the depth of the screw channel decreases gradually and the pressure rises; this section also completes the melting of the material begun in the previous section. (3) The metering section or the melt conveying section, where the material is heated, subjected to high shear rates, and the pressure increased further. The throughput, or the volume flow rate of the material out of the die, is mainly controlled by this section.

In one of the earliest studies on the flow in a single screw extruder, Griffith [5] solved the governing equations for the flow of an incompressible fluid through a screw extruder, with the velocity and the temperature profiles taken as essentially the same as those in a channel of infinite width and length. Zamodits and

† Present address: IBM Corp., Endicott, NY 13760, U.S.A.
‡ Author to whom all correspondence should be addressed.

NOMENCLATURE

b	temperature coefficient of viscosity, equation (4)
b_m	$B_m(c_{mi}-c_{m0})$
B_m	moisture coefficient for viscosity
c_m	moisture concentration
c_{mi}	initial moisture concentration
c_{m0}	ambient moisture concentration
c^*	dimensionless c_m
C	specific heat of the fluid
D	mass diffusivity of moisture into the bulk material
D_b	barrel diameter
G	Griffith number, $\bar{\mu}V_{bz}^2/k(T_b-T_i)$
H	height of the screw channel
k	thermal conductivity of the fluid
L	axial screw length
n	power law index, equation (4)
N	screw speed [rev min^{-1}]
p	pressure
$\bar{p}$	reference pressure, $\bar{\mu}V_{bz}/H$
p^*	dimensionless pressure
Pe	Peclet number, $V_{bz}H/\alpha$
q_v	dimensionless volumetric flow rate (throughput)
Q	total volumetric flow rate
S	dimensionless sink term for moisture
S'	rate of reaction
t	time
$\bar{t}$	average residence time
T	temperature
T_b	barrel temperature
T_i	inlet temperature
u	velocity component in the x-direction
v	velocity component in the y-direction
V_b	tangential barrel velocity, $\pi D_b N/60$
V_{bx}	component of V_b along x, $V_b \sin(\phi)$
V_{bz}	component of V_b along z, $V_b \cos(\phi)$
w	velocity component in the z-direction
W	width of the screw channel
x	coordinate axis normal to screw flights
y	coordinate axis normal to the screw root
z	coordinate axis along the screw channel.

Greek symbols

α	thermal diffusivity, $k/\rho C$
β	dimensionless T_b, T_b/T_i
β_1	dimensionless b, b/T_i
$\dot{\gamma}$	strain rate
$\dot{\gamma}_0$	reference strain rate, equation (4)
$\dot{\gamma}^*$	dimensionless strain rate
θ	dimensionless temperature, $(T-T_i)/(T_b-T_i)$
μ_0	reference viscosity, equation (4)
$\bar{\mu}$	average viscosity, $\mu_0[V_{bz}/H\dot{\gamma}_0]^{n-1}$
ρ	density of the fluid
τ	shear stress
ϕ	screw helix angle.

Subscripts

b	barrel
dev	developed
s	screw
0	reference quantity.

Superscript

*	dimensionless quantity.

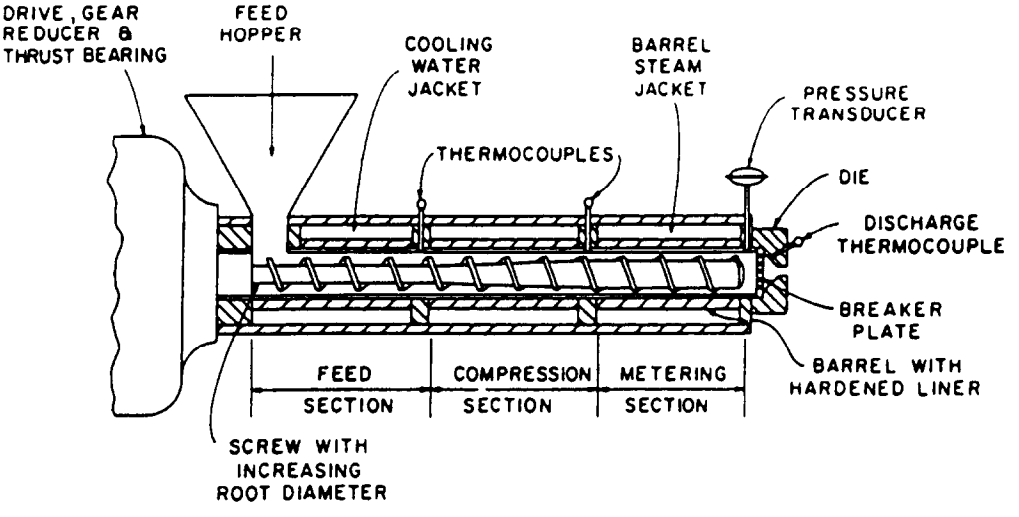

FIG. 1. Schematic of a single screw extruder.

Pearson [6] obtained numerical solutions for a fully developed, two-dimensional, isothermal flow of polymer melts in very wide rectangular screw channels. Rauwendaal [7] and Lappe and Potente [8] discussed the relationship between the volume flow rate and the pressure for single screw extruders.

Several researchers have studied the flow of polymers in the various sections of an extruder, using different numerical or analytical techniques [9–12]. Fenner [12] considered the case of the temperature profile developing along the length of the screw channel. Elbirli and Lindt [13] reported the results from a model in which the temperature was allowed to develop along the screw channel. Agur and Vlachopoulos [14] included models for the feed hopper, solid conveying and melt zones of the extruder. They also predicted the die swell that occurs as the material exits through a die. In these models, the screw and the barrel were assumed to be at the same, uniform temperature. Numerical results on the flow and heat transfer for polymeric materials in single screw extruders with an adiabatic boundary condition at the screw are presented in ref. [15]. This is a more realistic circumstance, since the screw is generally unheated. The flow field and the temperature distribution were shown to be affected significantly by the throughput in the extruder. Viscous dissipation was shown to be a very large effect and to result in heat transfer from the fluid to the barrel wall for certain materials and operating conditions.

Very few investigators have attempted to solve for the flow of food materials in a single screw extruder. Generally, food materials are assumed to have a rheological behavior similar to that of polymers. In reality, the material being processed exhibits elastic and time-dependent rheological properties. The elastic nature of the material manifests itself in the form of expansion or die swell after the material exits the die. Inside the extruder, however, the viscous contribution will be much higher than the elastic component because of the high shear and pressures that are built up. For the purposes of this simulation, therefore, a power-law type viscous material with variable viscosity is assumed. Bruin *et al.* [16] have considered the flow of biopolymers in an extruder. Harper [17] has discussed various aspects of food extrusion in single screw extruders. Recently, Mohamed and Morgan [18] have presented the results for average heat transfer coefficients in a single screw extruder, for the flow of non-Newtonian food materials.

The above, brief, review of the relevant literature points out the need for a broad-based approach to the modeling of the combined effects of flow, heat and mass transfer in extrusion. Our motivation in carrying out this analysis is to fill the gap in terms of obtaining useful solutions to engineering problems in the design of extruders, while trying to gain an understanding of the fundamental physical mechanisms that underlie the above phenomena [19]. By making suitable simplifications to the geometry and by making reasonable assumptions based on scaling, quantitative results are obtained for the various quantities of interest in the coupled problem of flow, heat and mass transfer with chemical reactions.

A finite difference numerical study has been carried out for the simulation of the transport processes in extrusion, to obtain the velocity, temperature and moisture concentration variation along the length of the screw channel. The analysis presented here is applicable largely to the metering zone where the cross-sectional area remains constant. However, the variation in channel depth due to taper may easily be accounted for in the model, in order to consider other regions in the extruder. The effects of viscous dissipation and chemical reaction are included and the results obtained are discussed in terms of the basic transport processes. The main governing dimensionless parameters are the throughput, or volume flow rate, q_v, the Peclet number Pe, which represents the relative importance of convection along the screw channel as compared to conduction, the power-law index n, the dimensionless viscosity coefficients β, β_1 and b_m, which characterize the variation of viscosity with temperature and moisture concentration, the dimensionless reaction rate S, and the Griffith number G, which represents the level of viscous dissipation as compared to heat conduction. The effect of these parameters on the flow, heat transfer and moisture distribution within the screw channel is studied in detail. It is found that the pressure developed at the die is strongly affected by the throughput and the power-law index. The residence time distribution is not significantly affected by changes in these parameters for the extruder geometry considered. The heat transfer at the barrel and the mixing induced in the flow are also investigated. It is found that the throughput is the most important parameter in the problem and affects the flow field very substantially, resulting in a strong influence on the heat and moisture transport as well.

2. PROBLEM FORMULATION

The simplified geometry of a single screw extruder and the cross section of a screw channel are shown in Fig. 2. For ease of visualization and analysis, the coordinate system is fixed to the screw root and, thus, the barrel moves in a direction opposite to the screw rotation. Such a formulation is commonly employed in the literature [2, 3]. As mentioned earlier, the analysis applies to the metering section of the screw extruder. Curvature effects are important in sections with deep channels, such as the solid conveying zone. However, for the shallow metering section modeled here, curvature effects are neglected. This allows the screw channel to be 'opened out', resulting in the rectangular computation domain shown in Fig. 3. For steady, developing, two-dimensional flow of a homogeneous fluid in a single screw extruder with a shallow channel, i.e. for $H \ll W$ in Fig. 2, after

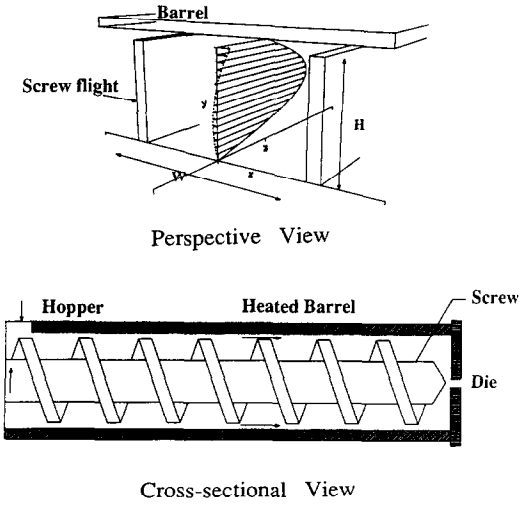

FIG. 2. Simplified geometry of a single screw extruder with a rectangular screw profile.

neglecting the inertia terms (creeping flow approximation [20]) in the x- and z-directions, the equations for the conservation of momentum become

$$\frac{\partial p}{\partial x} = \frac{\partial(\tau_{yx})}{\partial y}, \quad \frac{\partial p}{\partial y} = 0,$$
$$\frac{\partial p}{\partial z} = \frac{\partial(\tau_{yz})}{\partial y} \tag{1}$$

where p is the local pressure and τ the shear stress. The creeping flow approximation is valid because the inertia terms are small in comparison with the viscous terms for the low Reynolds numbers (typically 0.001) that arise for the highly viscous flow of polymer and food materials. The clearance between the screw flight and the barrel is assumed to be small enough to neglect the leakage across the flights from one screw channel to the neighboring one.

In the presence of strong viscous dissipation effects and/or heat addition from the barrel, the thermal convection along the channel length can be significant. Therefore, the temperature field is not fully developed in this direction. The velocities will also change with the downstream position as a result of this change in temperature, if the fluid viscosity is dependent upon its temperature. Also, the flow field may develop in the z-direction, depending on the flow entering the heated zone of the extruder channel. It is assumed that diffusion in the z-direction is negligible in comparison with convection. This assumption can be shown to be valid for $L \gg W$, using a simple scaling analysis, and is also borne out by experimental data. The temperature gradient in the y-direction is expected to be much higher than that in the down-channel direction. The diffusion term in the y-direction is, therefore, retained. Thus, the energy equation becomes [21]

$$\rho C w \frac{\partial T}{\partial z} = \frac{\partial}{\partial y}\left(k \frac{\partial T}{\partial y}\right) + \tau_{yx} \frac{\partial u}{\partial y} + \tau_{yz} \frac{\partial w}{\partial y} \tag{2}$$

where T is the temperature, ρ the density, C the specific heat at constant pressure and k the thermal conductivity of the fluid.

The above equation is parabolic in the z-direction

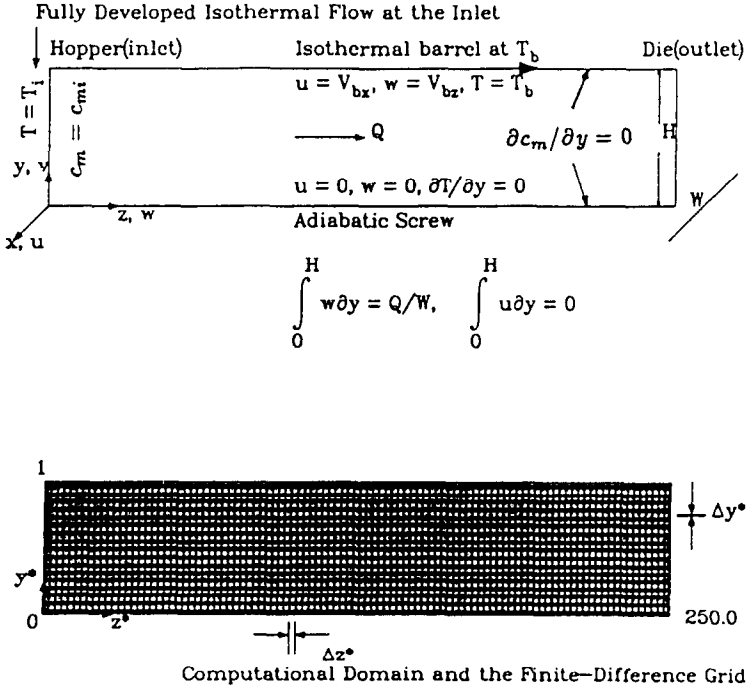

FIG. 3. Boundary conditions for the numerical model, employing a coordinate system fixed to the screw.

and elliptic in the y-direction. In actual practice, there is a restriction to the flow in the form of a die at the end of the extruder. The characteristics of the flow in the extruder are strongly coupled to that inside the die. The relationship among the flow quantities for the flow through dies has been studied, and correlations have been obtained [22]. For small throughputs, there is back flow, and this makes the problem elliptic in the z-direction also. In such circumstances, the fluid flow and the heat transfer at the die also need to be simulated and coupled to the extruder simulation. The present study is, however, restricted to the simulation of the transport phenomena in the extruder channel. The results obtained using this analysis can be used in conjunction with the characteristics of specific die shapes to obtain the operating characteristics of real extruders. The parabolic nature of the governing equation in the z-direction allows the use of a marching scheme [23], as described in the next section.

The shear stresses τ_{yx} and τ_{yz} are given by

$$\tau_{yx} = \mu \frac{\partial u}{\partial y}, \quad \tau_{yz} = \mu \frac{\partial w}{\partial y} \tag{3}$$

where μ is the molecular viscosity of the material. For non-Newtonian fluids, μ is a function of the strain rate $\dot{\gamma}$. A power law model is assumed in this study. An Arrhenius dependence of μ on the temperature T, and an exponential dependence on the moisture concentration c_m is also considered. Such a characterization of the viscosity variation with temperature and moisture content has been observed to accurately predict rheological measurements of typical food materials, as obtained experimentally by Kokini [24], among others. The following constitutive equation for viscosity is used:

$$\mu = \mu_0 \left(\frac{\dot{\gamma}}{\dot{\gamma}_0}\right)^{(n-1)} e^{b/T} e^{-B_m(c_m - c_{m0})} \tag{4}$$

where

$$\dot{\gamma} = \left[\left(\frac{\partial u}{\partial y}\right)^2 + \left(\frac{\partial w}{\partial y}\right)^2\right]^{1/2}. \tag{5}$$

Here, u and w are the velocity components in the x- and z-directions, respectively, b the Arrhenius temperature coefficient of viscosity, B_m the moisture concentration coefficient, n the power law index and subscript '0' denotes the reference conditions.

The mass diffusion equation also needs to be considered in addition to the continuity, momentum and energy equations for food systems because of the presence of moisture. Moisture plays a very important role in the extrusion of food materials. Similarly, for polymers, the species diffusion equation is relevant for systems with more than one constituent. In food systems, for example, some of the important effects of moisture transport are manifested in the form of gelatinization of the granular starch-based food material which is fed into the hopper of the screw extruder. This reaction occurs between the starch granules and the water molecules. Atwell *et al.* [19] defined starch gelatinization as the disruption of molecular orders within the starch granule that manifests itself in irreversible changes in the properties. In this study, for the modeling of moisture diffusion, gelatinization is defined as the process by which water gets bonded to the starch granules in the food material and thus becomes unavailable for further diffusion and transport. The mass diffusivity of bound moisture is reduced by several orders of magnitude and the food material is said to undergo a form of transition.

It has also been observed [17] that even small changes in the moisture content can result in large changes in viscosity. Besides, the moisture transport can also be affected by the reactions taking place during extrusion cooking. There is, thus, a need to consider this additional transport process in the modeling. The convection, diffusion, and absorption of moisture is governed by the following mass transport equation, valid for small values of the species concentration [21]:

$$w \frac{\partial c_m}{\partial z} = D \frac{\partial^2 c_m}{\partial y^2} + S'(c_m - c_{m0})^m; \quad S' = 0 \quad \text{for } T < T_{gel}. \tag{6}$$

Axial diffusion is neglected in comparison with the diffusion along the channel depth, as in the energy equation. The presence of vents or ports along the barrel sections is not taken into account. The coupling of this equation with the energy and momentum equations occurs via the dependence of viscosity on moisture content. The last term on the right-hand side of the equation represents a source/sink for moisture due to reaction. This term is modeled specifically to account for the absorption of moisture resulting from the gelatinization reaction in food systems that include starch. This term becomes operative only when the temperature exceeds the temperature needed for the onset of the gelatinization reaction, T_{gel}.

The complex structural changes that take place during gelatinization result in the loss of free moisture at a rate which depends on the prevailing moisture concentration, shear rate and temperature. A simple representation of this process is in the form of a chemical reaction rate term with reaction order m, as given above. Based on experimental observations [25], a first-order reaction ($m = 1$) is considered in this study. The proportionality constant is a function of the temperature and the shear rate, but is taken as constant in this study as a first approximation due to the paucity of data on the chemical kinetics. Recent experimental evidence suggests that at low temperatures, the shear effect is more dominant than the thermal effect [26]. Simulations using zeroth-order kinetics were also carried out, but the results are not presented here. There is some recent work [27] on the thermal kinetics aspects of starch gelatinization, which can be

combined with appropriate shear kinetics models in order to realistically simulate the entire process.

The boundary conditions are prescribed as shown in Fig. 3. The screw has been taken as isothermal, at T_b, in most studies reported in the literature. However, a more practical circumstance is represented by the adiabatic condition at the screw surface [15]. Experimental evidence lends support to this assumption. Otherwise, a conjugate problem needs to be examined where the conduction in the screw is coupled to the conduction and convection inside the flow channel.

Two constraints arise on the basis of flow rate conservation considerations. If the leakage flow across the screw flights is taken as negligible, these constraints are given, for a total volumetric flow rate Q, by

$$\int_0^H u\,dy = 0, \quad \int_0^H w\,dy = \frac{Q}{W}. \tag{7}$$

The governing equations are nondimensionalized in terms of the following dimensionless variables:

$$x^* = x/H, \quad y^* = y/H, \quad z^* = z/H$$

$$u^* = u/V_{bz}, \quad w^* = w/V_{bz}$$

$$p^* = \frac{p}{\bar{p}}, \quad \bar{p} = \bar{\mu}\frac{V_{bz}}{H}, \quad \theta = \frac{T-T_i}{T_b-T_i}$$

$$c^* = \frac{c_m - c_{m0}}{c_{mi} - c_{m0}}, \quad b_m = B_m(c_{mi} - c_{m0})$$

$$\beta = T_b/T_i, \quad \beta_1 = b/T_i$$

$$\dot{\gamma}^* = \frac{\dot{\gamma}H}{V_{bz}}, \quad \bar{\mu} = \mu_0\left[\frac{V_{bz}/H}{\dot{\gamma}_0}\right]^{n-1}$$

$$Pe = V_{bz}H/\alpha, \quad G = \frac{\bar{\mu}V_{bz}^2}{k(T_b - T_i)}$$

$$Le = D/\alpha, \quad S = S'H^2(c_{mi} - c_{m0})^{m-1}/\alpha \tag{8}$$

where α is the thermal diffusivity, T_i the temperature of the flow at the inlet, Pe the Peclet number representing the effect of convection downstream in relation to conduction across the channel depth, Le the Lewis number representing the relative magnitude of moisture diffusivity to thermal diffusivity, and G the Griffith number denoting the importance of viscous dissipation effects. The parameters β and β_1 represent the dependence of viscosity on temperature and b_m represents the dependence on moisture concentration.

Our choice of the above dimensionless parameters is based partly on rigorous normalization of the governing equations and partly on physical reasoning derived from experimental knowledge. For instance, the operating parameters for an extruder include the flow rate, screw speed, and die geometry (for a given screw configuration). The parameter q_v represents a combination of the volumetric flow rate, screw speed and the channel depth (see equation (13) below). Thus, the flow rate q_v and the screw speed are not independent. This fact is reflected in our study by making appropriate changes in the parameters Pe and G for corresponding changes in screw speed.

The resulting dimensionless equations are

$$\frac{\partial p^*}{\partial x^*} = \frac{\partial}{\partial y^*}\left(\frac{\partial u^*}{\partial y^*}[\dot{\gamma}^*]^{(n-1)}\,e^{\beta_1/\{\theta(\beta-1)+1\}}\,e^{-b_m c^*}\right) \tag{9}$$

$$\frac{\partial p^*}{\partial z^*} = \frac{\partial}{\partial y^*}\left(\frac{\partial w^*}{\partial y^*}[\dot{\gamma}^*]^{(n-1)}\,e^{\beta_1/\{\theta(\beta-1)+1\}}\,e^{-b_m c^*}\right) \tag{10}$$

$$Pe\,w^*\frac{\partial\theta}{\partial z^*} = \frac{\partial^2\theta}{\partial y^{*2}} + G[\dot{\gamma}^*]^{(n+1)}\,e^{\beta_1/\{\theta(\beta-1)+1\}}\,e^{-b_m c^*} \tag{11}$$

$$Pe\,w^*\frac{\partial c^*}{\partial z^*} = Le\frac{\partial^2 c^*}{\partial y^{*2}} + Sc^{*m}; \quad S = 0 \quad \text{for } \theta < \theta_{gel}. \tag{12}$$

Similarly, the boundary conditions are also obtained in dimensionless form. The constraints on the flow are obtained, in dimensionless form, as

$$\int_0^1 u^*\,dy^* = 0, \quad \int_0^1 w^*\,dy^* = q_v = \frac{Q/W}{HV_{bz}}. \tag{13}$$

Here, the parameter q_v represents the dimensionless volumetric flow rate, generally referred to as the throughput, emerging from the extruder. It is related in a complex manner to the presence of a die at the end of the extruder.

Thus, for a given screw configuration, the parameters that govern the problem are the Peclet number Pe, the Griffith number G, the throughput q_v, the dimensionless sink term S for moisture, the Lewis number Le, the dimensionless reaction temperature θ_{gel}, the viscosity parameters β, β_1, b_m, and the power law index n.

3. SOLUTION PROCEDURE

The governing equations derived above constitute a coupled set of non-linear partial differential equations, the coupling arising mainly through the viscosity which is a function of the temperature and the moisture concentration. Analytical solutions are difficult to obtain even for simple cases, and therefore, a numerical procedure is used here.

The dimensionless equations are solved by means of finite difference techniques. The computations were carried out over $y \times z$ grid sizes of 41×101, 61×101 and 81×101. The results were essentially unchanged when the grid was refined to 81×121 from 61×101 and therefore, a 61×101 grid was selected. Since the energy and moisture transport equations, equations (11) and (12), are parabolic in z, boundary conditions are necessary only at $z = 0$ to allow marching in the z-direction and, thus, obtain the solution in the entire domain. It is assumed that there is no significant back flow. For situations where there is significant back

flow, the marching procedure is not applicable. The throughput parameter q_v determines the limits of applicability of the marching scheme. As a rough estimate, a value of q_v less than 0.18 resulted in significant back flow, for typical values of the other parameters, limiting the use of marching for the numerical solution.

A method similar to the one developed by Fenner [3] was employed for solving the momentum equations, equations (9) and (10), at a given z location iteratively. These equations are integrated twice over y^*. The following four non-linear equations are obtained after applying the boundary conditions for u and w at the screw root and the barrel:

$$\partial p^*/\partial z^* = (J_0 - J_1 - J_0 q_v)/(J_0 J_2 - J_1^2) \quad (14a)$$

$$(\partial p^*/\partial z^*) y_0^* = (J_1 - J_2 - J_1 q_v)/(J_0 J_2 - J_1^2) \quad (14b)$$

$$\partial p^*/\partial x^* = (J_0 - J_1)\tan\phi/(J_0 J_2 - J_1^2) \quad (14c)$$

$$(\partial p^*/\partial x^*) y_1^* = (J_1 - J_2)\tan\phi/(J_0 J_2 - J_1^2) \quad (14d)$$

where y_0^* and y_1^* are the y locations in the channel (from the screw root to the barrel) where the shear stresses are zero.

In the above equations

$$J_m = \int_0^1 \alpha^m F(\alpha)\, d\alpha \quad (15)$$

with

$$F(y^*) = [(\partial p^*/\partial x^*)^2 (y^* - y_1^*)^2 + (\partial p^*/\partial z^*)^2 (y^* - y_0^*)^2]^{(1-n)/2n} e^{-\beta_1/[n(\theta(\beta-1)+1)]} e^{b_m c^*/n}. \quad (16)$$

Equations (14a)–(14d) need to be solved iteratively by starting with reasonable guesses for both the pressure gradients $\partial p^*/\partial z^*$, $\partial p^*/\partial x^*$, and for y_0^*, y_1^*. The Newton–Raphson iteration scheme is employed. The Gauss–Jordan algorithm is used for solving the system of equations that are obtained [23]. The iterations are terminated when the pressure gradients satisfy the following convergence criterion:

$$\max[\Delta(\partial p^*/\partial z^*),\ \Delta(\partial p^*/\partial x^*)] \leqslant 10^{-4} \quad (17)$$

where Δ stands for the absolute value of the fractional change between two consecutive iterations. This particular convergence criterion is not useful when the values of the pressure gradients become very small, i.e. close to zero. Under such circumstances, only the absolute change in the values of the pressure gradient is considered for convergence. Values of the criterion smaller than 10^{-4} were also tried, and it was found that satisfactory convergence was obtained with the above value within a reasonable number of iterations (typically 5–10). A different method was used in ref. [15] to solve the momentum equations. The two schemes give essentially the same results for pressure rise along the extruder. However, the scheme in ref. [15] is restricted to a narrower range of q_v.

Using the boundary conditions, in terms of u^*, w^*, θ and c^* at any upstream z location, the energy equation, equation (11), is solved to obtain the temperature distribution at the next downstream z location. Equation (11) is solved using the fully implicit scheme [23]. In this scheme, a tridiagonal system of equations is obtained by using the new, uncalculated, values of the dependent variable from the differencing operation in the y-direction at any nodal point in the numerical scheme. The tridiagonal system is solved using the well-known Thomas (TDMA) algorithm, which is very efficient [28]. The moisture transport equation, equation (12), is solved next using, once again, the fully implicit scheme to obtain the values of moisture concentration at the next location in the marching direction. With the temperature and moisture concentration distributions obtained at the next downstream location, the momentum equations, equations (9) and (10), are solved iteratively, as discussed above, to obtain the velocity distribution there. This procedure is repeated until the end of the extruder channel is reached. The integration in equation (15) was carried out numerically using Simpson's one-third rule [28].

3.1. *Typical parameter values*

For typical situations, corresponding to the extrusion of a polymeric/food material, and for typical throughputs and screw speeds, the following values of the dimensionless parameters are chosen to represent a typical extruder and typical operating conditions:

Power-law index	n	0.5
Throughput	q_v	0.3
Peclet number	Pe	7000
Griffith number	G	10^{-3}
Barrel temperature parameter	β	1.1
Temperature coefficient of μ	β_1	10.0
Moisture coefficient of μ	b_m	1.0
Lewis number	Le	0.001
Gelatinization temperature	θ_{gel}	0.5
Moisture sink term	S	−10
Ambient moisture concentration	c_{m0}	0.0

Numerical results are obtained for wide ranges of the governing parameters, varying them from these typical values. Some characteristic results are presented in the next section.

4. RESULTS AND DISCUSSION

Results are presented in terms of distributions of velocity, temperature and moisture concentration along the screw channel as well as across the channel depth. An important measure of the performance of the extruder is its ability to pump the material through the die. The variation of pressure along the channel as a function of the governing parameters is useful in this regard, and is examined here. Other quantities of practical interest, such as the bulk temperature and residence time distribution, are derived from the pro-

files. Contour plots of constant velocity, temperature and moisture are also obtained. The coordinate system is fixed to the screw as described earlier. For ease of discussion and presentation of results, some of the parameters are kept constant while the others are changed to study their effect on the transport processes. For the results presented here, the following are kept constant: $Pe = 7050$, $Le = 0.001$, $\theta_{gel} = 0.5$, $c_{m0} = 0.0$, $\phi = 16.54^{\circ}$ and $\beta = 1.134$. In addition, the calculations are carried out for $\beta_1 = 10$ and $b_m = 1$. These values are typical of the conditions for the extrusion of starches. Other values of these parameters were also considered, but those results are not reported here for brevity.

Figure 4(a) shows the calculated isotherms and the temperature profiles at four downstream locations for a non-Newtonian fluid with $n = 0.3$. The parameter G, which represents the relative importance of viscous dissipation as compared to heat conduction in the y-direction, is quite high and gives rise to fluid temperatures that are higher than the barrel temperature, i.e. θ larger than 1. Consequently, heat transfer occurs from the fluid to the barrel which may, therefore, have to be cooled in the sections close to the die in order

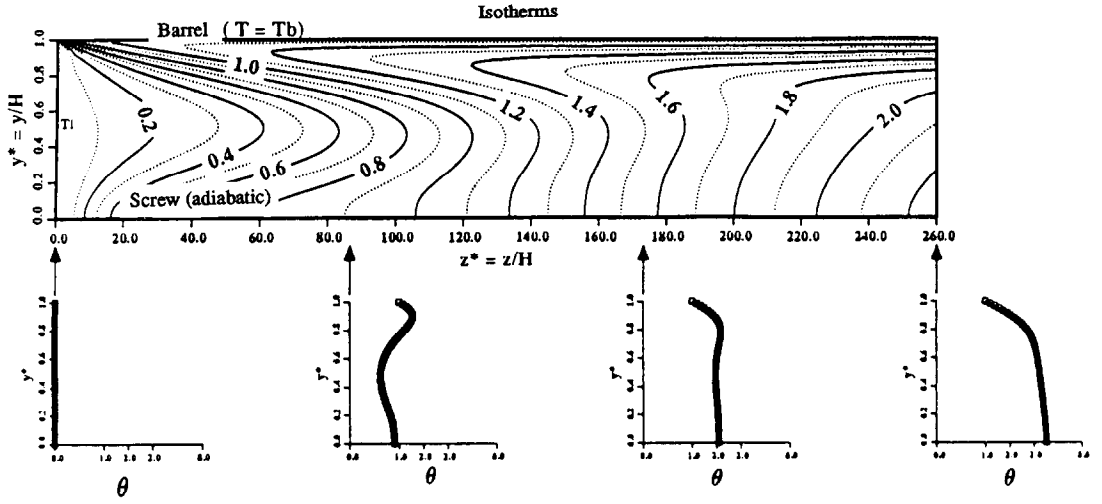

a) Temperature Profiles

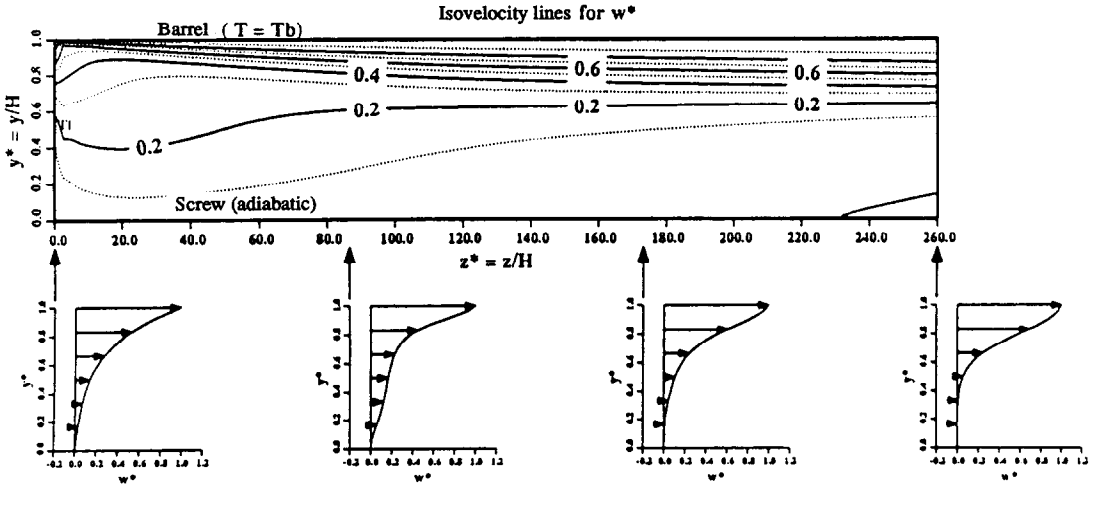

(b) Velocity Profiles

FIG. 4. (a) Isotherms and temperature profiles, and (b) velocity profiles at four downstream locations for a non-Newtonian fluid with $n = 0.3$, $\phi = 16.54^{\circ}$, $q_v = 0.25$, $Pe = 7050$, $G = 0.005$, $\beta = 1.134$, $\beta_1 = 10.0$, $b_m = 1.0$, $S = -1000$, $Le = 0.001$, $\theta_{gel} = 0.5$.

to maintain it at a particular temperature. For smaller values of G, the more common situation of heat transfer from the barrel to the fluid arises. The temperature gradient, $\partial T/\partial y$, at the barrel is also higher than that at the screw root because the heat generated by viscous dissipation has to be conducted away from the barrel to the ambient, whereas the screw root is adiabatic. Uniformity of properties in the product is an important attribute in the design of extruders which are used for the thermal processing of temperature-sensitive non-Newtonian materials. The presence and location of hot spots in the material can be judged by the occurrence of large temperature gradients close to the source of hot spots. The shape of the isotherms and the spacing between them can thus provide guidelines in the design of extruders to avoid such isolated, hot regions.

Figure 4(b) shows constant velocity lines and four down-channel velocity profiles for the conditions mentioned above. The dimensionless down-channel velocity is zero at the screw root and unity at the barrel for the barrel-moving formulation considered here. The velocity profile does not change significantly from one z location to the next. The steamlines are uniform and parallel to the z coordinate for this case of negligible back flow. A different set of conditions is considered in Figs. 5(a) and (b) in order to examine the development of the flow and thermal fields in greater detail. The throughput in Fig. 5 is very large ($q_v = 0.5$) and the material is non-Newtonian with $n = 0.3$. The velocity profiles indicate that the flow develops from the initially linear profile as in drag flow to a more complex one based on the temperature field. The viscous dissipation contribution is still quite large, but the temperature values do not reach the high values seen in Fig. 4 because of the high flow rate. It may also be noted that the slower fluid near the screw root gets heated to higher temperatures than the fluid near the barrel due to viscous heating.

Figure 6 shows the moisture concentration contours. As shown here, the effect of the sink term, S, due to the reaction, is manifested in a decrease in the moisture concentration due to bonding of water for gel formation as the material reaches the gelatinization temperature θ_{gel}. This loss of moisture occurs at a rate specified by the sink term S and is obviously more rapid for larger S. As the sink term is increased in magnitude from $S = 0$, i.e. no reaction, the sharp decrease in the moisture concentration occurs first at the screw root. These results may also be compared with those in Fig. 7 for the case when $S = -500$. The two variables that control the magnitude of viscosity, i.e. the temperature and the moisture concentration, act in opposing directions as the material gets heated up and loses moisture due to gelatinization. The temperature profiles indicate that the screw root gets hotter than the barrel wall for the set of conditions shown in the figure, and this leads directly to gelatinization near the screw first. In actual practice, however, the screw is in motion and the barrel is stationary. The material at the screw root and at the barrel is not transported downstream and is, therefore, exposed to the prevailing temperatures and shear rates. The sink term must strictly account for this fact by means of a functional dependence of S on the prevailing shear rate. This study has examined the effect of S parametrically, without assuming an arbitrary functional dependence. Nevertheless, the physical reasoning presented here is valid.

Once the moisture concentration decreases sharply due to the reaction, the viscosity level is controlled by the relative magnitude of the decrease due to the temperature rise and the increase due to moisture removal. The downsteam distribution of moisture concentration and the pressure development are now based on the usual transport processes, but with altered viscosity and a non-uniform moisture level along the channel depth. The pressure at the end of the extruder and the quantity of initial moisture remaining after extrusion both depend on the location at which the reaction starts. This phenomenon is discussed below for the pressure rise.

Figure 8 shows the effect of varying the strength of the sink on the pressure rise along the channel. As compared to the case of $S = 0$, the dimensionless pressure at the die is seen to be lower for higher sink strengths. The variation of the downstream pressure gradient (not shown here) with the channel length shows that there is a kink in the profile at the point where the gelatinization first occurs. However, this rise in the value of dp/dz is not strong enough to counter the temperature effect which tends to lower the viscosity and, thus, makes the material flow more easily reducing the pressure rise. In fact, for very high sink strengths ($S \approx -10\,000$), the pressure at the die is higher than the value obtained for $S = 0$ due to the resulting smaller moisture levels. These results are not discussed here because such high values of S are not of much practical significance.

Figure 9 shows the effect of changing the power-law index n of the material on the pressure obtained in the extruder channel. The curves are for $G = 0.001$, $q_v = 0.3$ and $S = -1000$. Thus, only n is varied keeping the rest of the terms in equation (4) the same. This implies a higher viscosity for higher n at a given shear rate. These results indicate the effect of n, though no actual physical circumstance is stimulated here. The pressure rises from the hopper to the die along the screw helix, as expected. The pressure gradient is higher for increasing n. For non-Newtonian fluids, $n < 1$ and the viscosity decreases with an increase in shear rate. The Newtonian fluid, $n = 1$, therefore, gives rise to larger viscous drag which in turn leads to larger pressure gradients required to overcome it.

A bulk temperature T_{bulk} is defined in order to quantify the combined thermal effect of viscous dissipation and barrel heating. It is based on the prevailing velocity and temperature fields, and is equivalent to the commonly used 'mixing cup' temperature. In physical

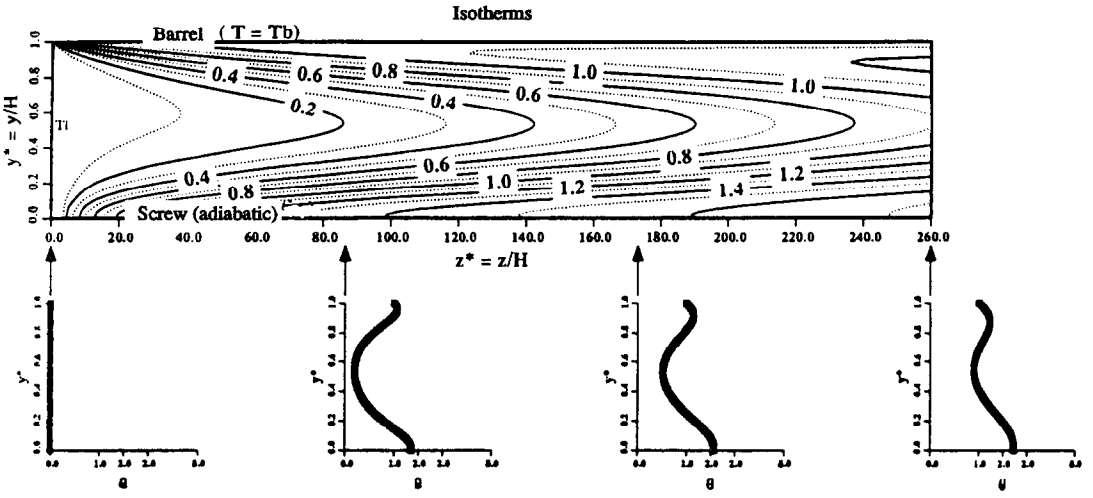

(a) Temperature Profiles

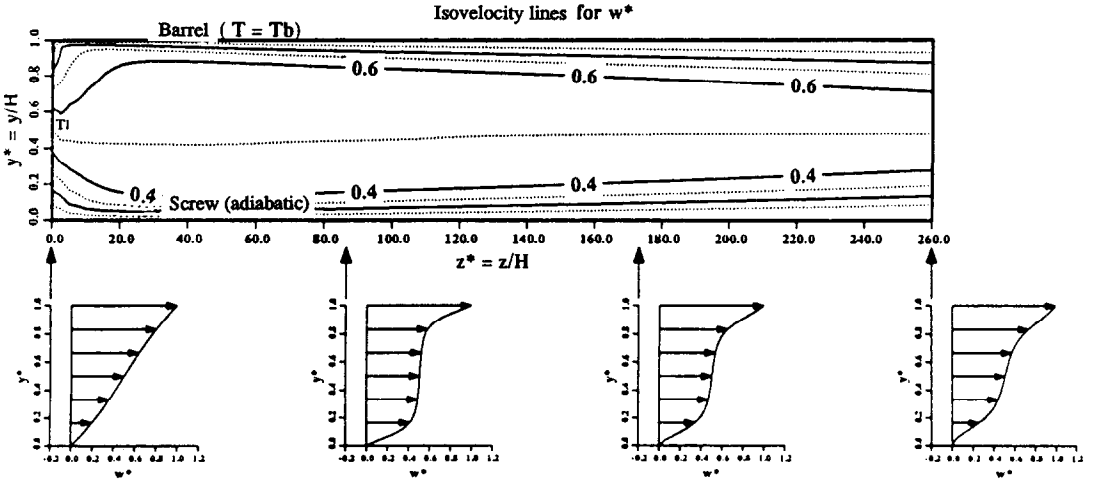

(b) Velocity Profiles

FIG. 5. (a) Isotherms and temperature profiles, and (b) velocity profiles at four downstream locations for $q_s = 0.5$, $G = 0.01$; other conditions as in Fig. 4.

terms, it represents the rate of convected energy per unit mass flow. Thus

$$T_{\text{bulk}} = \int_0^H wT\,dy^* \Big/ \int_0^H w\,dy^*. \tag{18}$$

The effect of viscous dissipation is examined in terms of T_{bulk} as defined above. Figure 10 shows the effect of the Griffith number G on the bulk temperature. As expected, a larger value of G results in greater bulk temperature rise. The contribution of the source term in the energy equation due to viscous dissipation results in temperatures that are much larger than the imposed barrel temperature. The bulk temperature increases continuously from the hopper to the die because the barrel is maintained at a uniform temperature while the material heats up due to viscous dissipation. Material temperatures higher than the barrel temperature cause heat transfer to take place from the material to the barrel wall, and consequently, it becomes necessary to cool the barrel in the sections close to the die, as mentioned earlier. The dimensionless bulk temperature at the die increases by about 200% for an increase of G from 0 to 0.005. In practical situations, however, an increase in G is brought about by a corresponding increase in the screw speed or other operating conditions. Hence, fixing the oper-

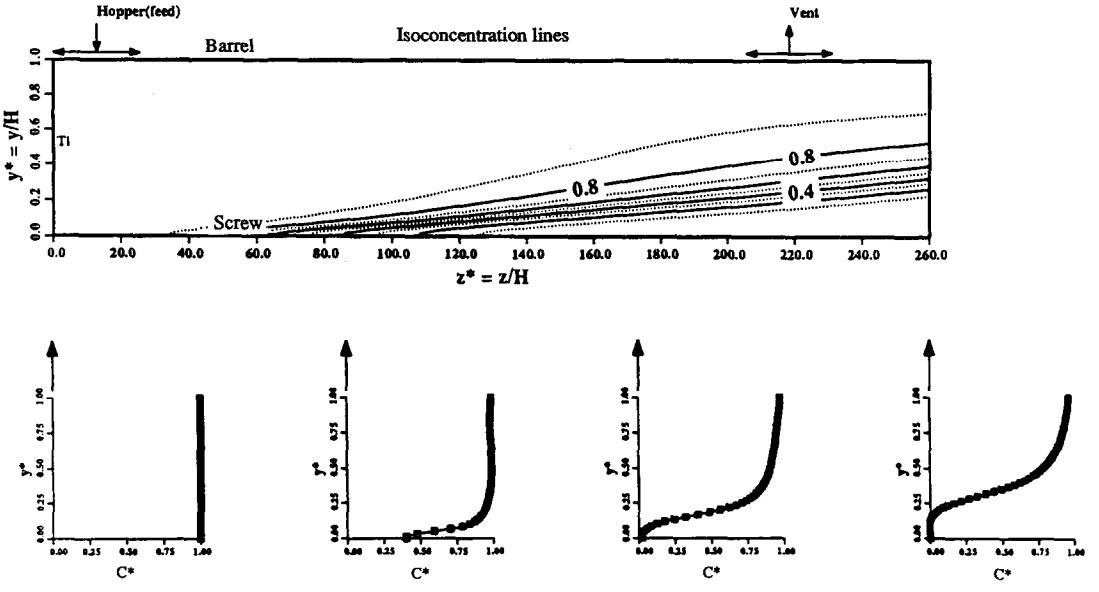

FIG. 6. Lines of constant moisture concentration c^*, along with the corresponding profiles, at four downstream locations for the conditions given in Fig. 4.

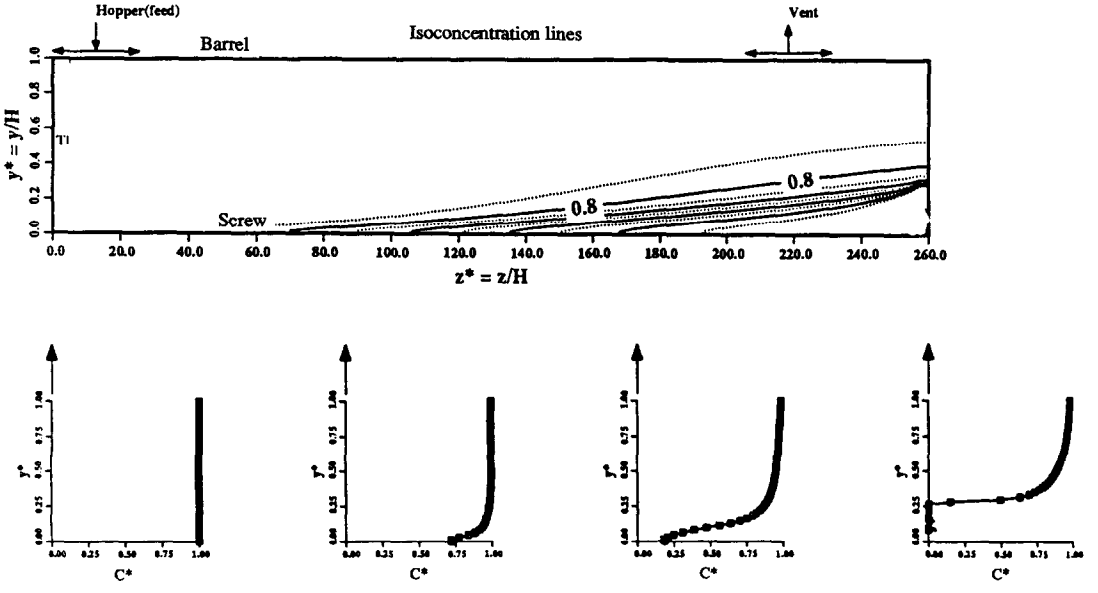

FIG. 7. Lines of constant moisture concentration c^*, along with the corresponding profiles, at four downstream locations for $S = -500$; other conditions as in Fig. 4.

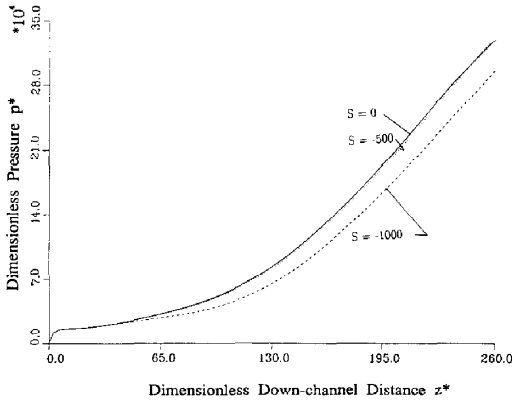

FIG. 8. Effect of the strength of the moisture sink S on the variation of the dimensionless pressure p^* along the screw channel length z^* for the conditions given in Fig. 4.

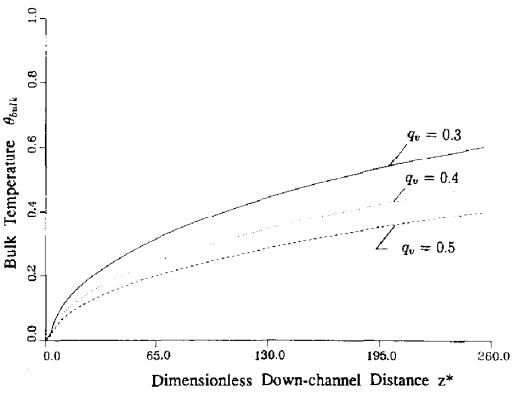

FIG. 11. Effect of the throughput q_v on the variation of bulk temperature along the screw channel length z^* for $n = 0.5$, $G = 0.0$, other conditions as in Fig. 4.

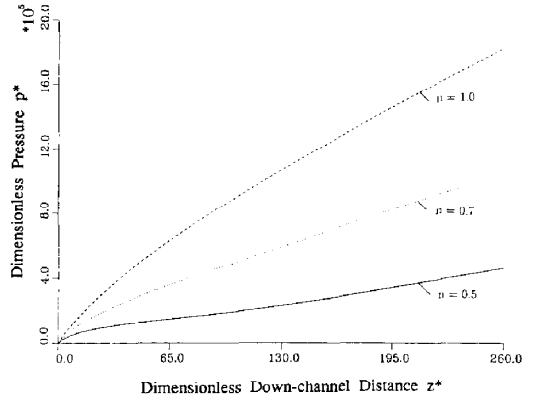

FIG. 9. Effect of the power-law index n on the variation of dimensionless pressure p^* along the screw channel length z^* for $q_v = 0.3$, $G = 0.001$, other conditions as in Fig. 4.

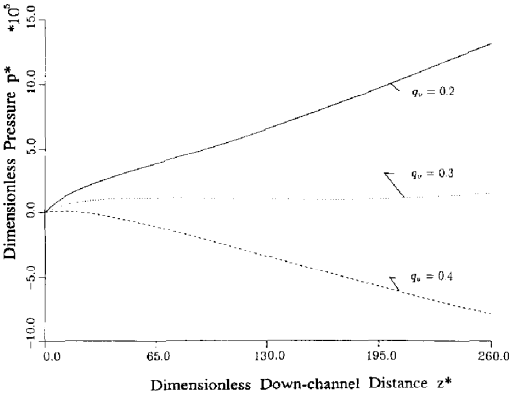

FIG. 12. Effect of the throughput q_v on the variation of dimensionless pressure p^* along the screw channel length z^* for $n = 0.5$, $G = 0.0$, other conditions as in Fig. 4.

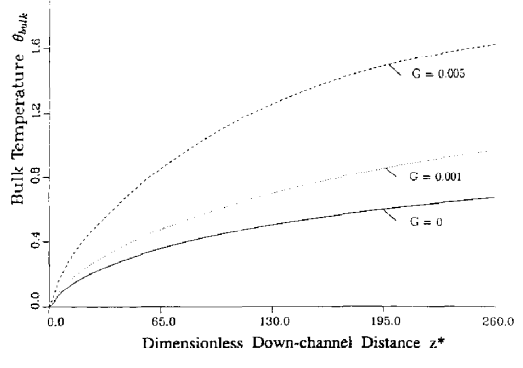

FIG. 10. Effect of the viscous dissipation parameter G on the variation of bulk temperature along the screw channel length z^* for the conditions given in Fig. 4.

ating conditions usually fixes the values of parameters such as G and Pe. The above discussion is valid only for a parametric variation of G.

When the throughput is changed, keeping the other parameters constant, the bulk temperature also changes as shown in Fig. 11. For increasing throughputs, the bulk temperature decreases as a function of the down-channel distance. This is because the average residence time for the material inside the extruder is reduced for higher q_v, thereby reducing the bulk temperature that it experiences. This change in θ_{bulk} is about 30% for a change in q_v from 0.3 to 0.5.

The effect of the throughput q_v on the pressure development at the die is investigated next. As shown in Fig. 12, a smaller value of q_v, which corresponds to greater restriction to the flow at the die, results in a larger pressure rise as compared to the case with $q_v = 0.4$, which is close to the open die situation for the isothermal flow of Newtonian fluids, $q_v = 0.5$ [15]. For the particular set of conditions considered here, a larger value of q_v results in pressure loss from the hopper to the die. This is because the balance between the pressure build-up as the material flows through the extruder channel, and the easing of pressure due to the decrease of viscosity, is not maintained. If the flow rate is increased, the pressure at the die decreases further. Therefore, there is a limiting value of the throughput q_v that can be fed through an extruder beyond which pressure development and, corre-

spondingly, the development of desirable material quality is affected considerably. This limiting value depends on the particular conditions governing the flow, for example, the power-law index n and the viscosity coefficients β, β_1 and b_m. For isothermal, Newtonian flow, a simple theoretical analysis shows that $q_v = 0.5$ corresponds to the throughput in the extruder in the absence of a die. For the non-isothermal, non-Newtonian flow considered here, this value for the no-die situation is difficult to estimate, but is typically around 0.3.

The residence time distribution (RTD) is another important characteristic of an extruder. An average residence time can be defined as the ratio of the total extruder volume to the volumetric flow rate. In addition, there is a distribution of time spent by the particles that start at different channel depths because of the variation in the downstream velocity with the y location. It is an indication of the amount of time the material spends within an extruder. If the material spends an excessive amount of time inside the extruder, it may have undesirable effects on the extrudate quality. The nature of the RTD curve can provide indications regarding blockage in the extruder channel, for example. An on-line monitoring of such information is useful in designing control systems that change the screw speed, throughput or other operating variables as and when necessary.

A numerical procedure [15] is used to calculate the RTD using particle traces and following the path of each particle as it moves from the inlet to the die. A fixed amount of dye is assumed to be introduced at the hopper. The time required for a dye particle to cover the distance L, i.e. axial screw length, is calculated from the axial component of the velocity at that (y, z) location. The cumulative amount of dye material that comes out of the extruder is plotted in Fig. 13 as a function of time. After an initial time interval, t_0, the first dye material starts coming out. Then, a large amount of material corresponding to particles in the intermediate depths comes out. Near the barrel and the screw, the axial component of the velocity is relatively small and therefore, that material spends a much larger time inside the extruder. The curve shown in Fig. 13 is a typical profile for extruders.

The numerical results obtained above were validated with experimental data. Experiments were carried out on a specially designed single screw extruder which is well instrumented. Details of the experimental set-up and measurements are given in ref. [29]. Only some of the typical results are presented here for comparison with the numerical results. Materials such as Heavy Corn Syrup, which is Newtonian, and Viscasil 300-M, which is non-Newtonian with $n \simeq 0.4$ and whose thermal properties have been characterized quite accurately [29], are fed into the extruder channel. These fluids do not undergo a phase change and the experiments are largely directed at the validation of the model developed, using these simpler fluids. The quantities of interest such as throughput, revolutions

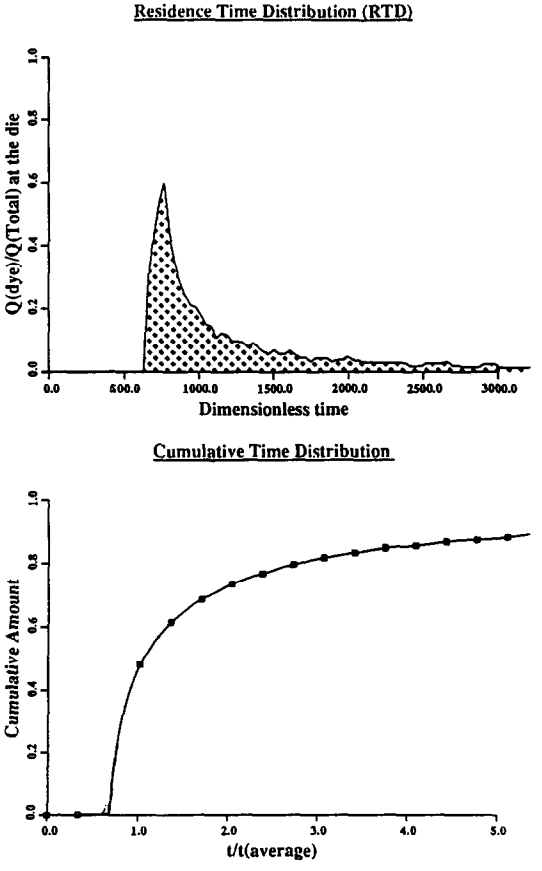

FIG. 13. Residence time distribution for the flow of a non-Newtonian fluid for the conditions given in Fig. 4.

per minute, pressure and temperature profiles are measured for a specific die at the end of the extruder. As shown in Fig. 14, the pressure–throughput characteristics for a 3.6 mm die match quite closely with the experimental data from the extruder. We have shown dimensional quantities in the figure for two reasons. (1) The dimensionless throughput q_v is a combination of the actual flow rate and the revolutions per minute, and each of the experimental data points corresponds to different values of these two variables. This leads to difficulty in showing the graph with q_v as the only variable. (2) An estimate of the physical magnitude of the pressure and the flow rate typically found in extruders can be obtained by examining the graph.

It is interesting to note that the actual screw channel profile in the experiments is not rectangular but has a more complex geometry known as the self-wiping profile [29]. Nevertheless, the rectangular profile approximation using the maximum channel depth is found to be quite sufficient for purposes of overall prediction. As an example, the computed and experimentally measured die pressure for the flow of corn syrup at a mass flow rate of 8.43 kg h^{-1}, at 35 rev min^{-1}, and the barrel maintained at 22.3°C, are 10.75

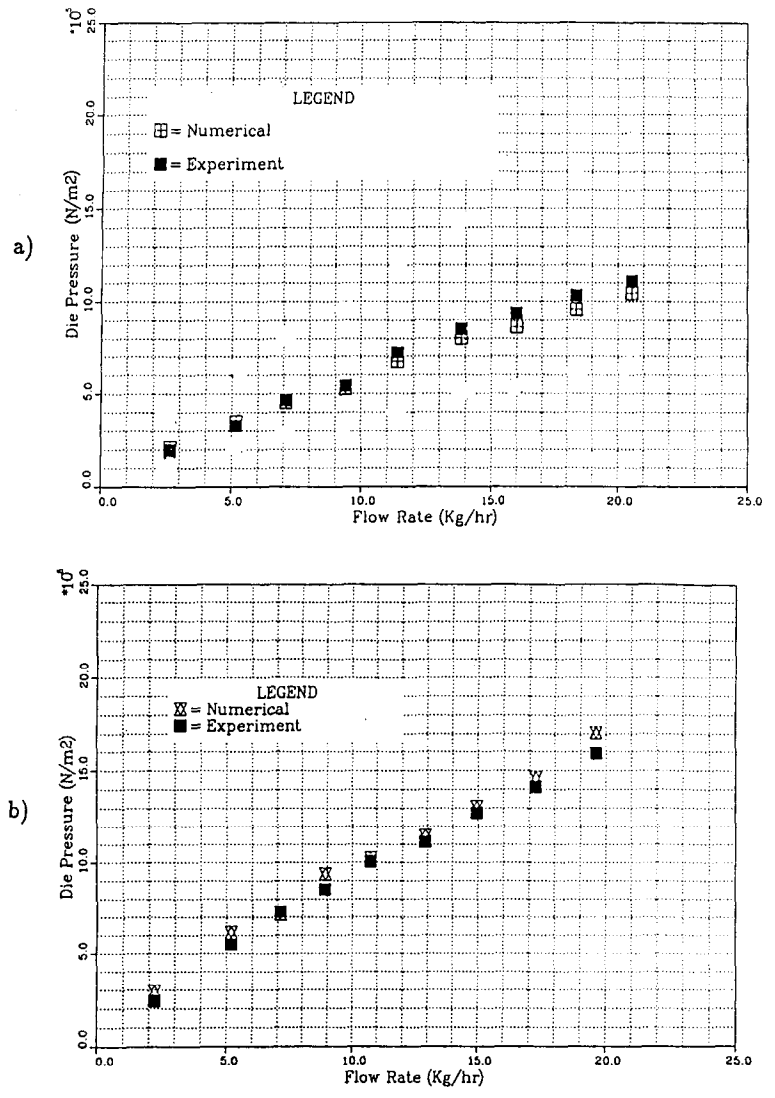

FIG. 14. Comparison of numerical and experimentally measured extruder characteristics in terms of the die pressure vs throughput for the flow of Corn Syrup in a single screw extruder; $T_b = 35°C$, $T_i = 25°C$: (a) die diameter = 3.6 mm; (b) die diameter = 2 mm.

and 11.34 bar, respectively. The corresponding bulk temperatures are 22 and 22.3°C. A different set of operating conditions (4.53 kg h^{-1}, 20 rev min^{-1}, barrel at 12.2°C) again shows excellent agreement (numerical/experimental die pressures are 22.65 and 20.4 bar, respectively).

Figure 15 demonstrates detailed temperature profile calculations and the comparison with experiments, using corn syrup. The experimental measurements were carried out with a uniquely designed cam-driven thermocouple probe which traverses the extruder channel from the barrel to the screw root (see ref. [29] for details). In this example, $y^* = 0$ corresponds to the screw root and $y^* = 1$ corresponds to the inner surface of the barrel. At the particular axial location (about two-thirds the total extruder length), the predicted profile matches fairly well with the experimentally measured profile. The discrepancy seen in Fig. 15(b) is explained as follows: the externally imposed barrel temperature at the given channel location is used as an input in the numerical calculations. However, in the experiment, this temperature at the barrel surface actually varies along the extruder axial length. A better fit to the experimental data is obtained if this actual variation of the barrel temperature is employed in the calculations. The use of an average barrel temperature over the extruder length under consideration also gives a better agreement. The maximum variation in temperature from the barrel to the screw root, however, is typically 1–2°C for these cases. The adiabatic condition at the screw root is also demonstrated quite well by the experimental data. These comparisons show that the numerical model predicts the trends and the physical phenomena

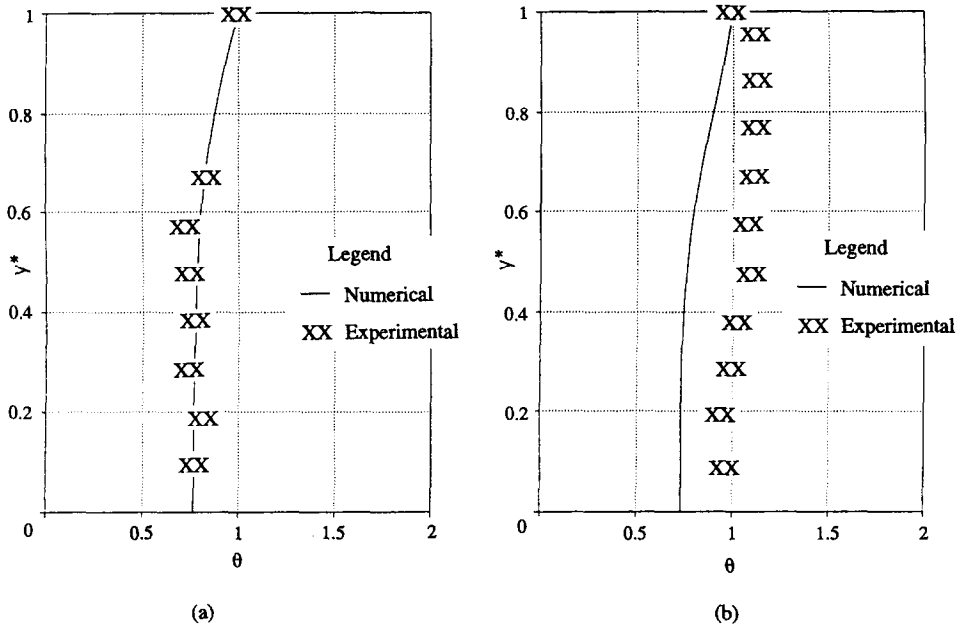

FIG. 15. Comparison of calculated temperature profiles in the screw channel with experimental data: (a) Corn Syrup, $N = 20$ rev min^{-1}, $T_b = 12.2°C$, $T_i = 21.2°C$; (b) Corn Syrup, $N = 35$ rev min^{-1}, $T_b = 23.5°C$, $T_i = 18.5°C$.

reasonably well, despite the simplifying assumptions made in the analysis. Thus, the results obtained are physically realistic and of good accuracy, allowing the use of the model for predicting transport phenomena within the extruder. Further work on a detailed experimental investigation of the temperature and velocity profiles in the extruder, for a variety of materials, is clearly needed. In particular, experimental data on realistic chemically reacting materials and more extensive inputs on the rheology and on the chemical kinetics are needed to improve the mathematical model discussed here and for a more appropriate validation. This effort is presently being carried out as part of the overall research project.

5. CONCLUSIONS

A numerical simulation of the transport phenomena occurring in the flow of a non-Newtonian fluid through a single screw extruder has been carried out. For significant viscous dissipation within the material, the material temperature rises above the imposed barrel temperature by as much as 100%. The bulk temperature at the die exit increases by almost 200% for a change in the viscous dissipation parameter G from 0 to 0.005. Moisture removal and bonding due to reaction takes place earlier and first at the screw root for higher reaction rates. The bonding takes place within a very short distance from the inlet, along the extruder channel, giving rise to sharp changes in viscosity at that location. Pressure development at the end of the extruder is significantly affected by the throughput. For throughputs larger than a limiting value, typically 0.3, the pressure can actually decrease from the hopper to the die, which means that the material has to be pumped through the extruder to maintain the given flow. Non-Newtonian behavior reduces the pressure developed at the die. The bulk temperature, which represents an overall effect of the thermal and flow history within the extruder, rises continuously from the hopper to the die. For the conditions examined here, the dimensionless bulk temperature becomes larger than 1, and nearly half the barrel section towards the die needs to be cooled in order to maintain it at a uniform temperature. The residence time distribution (RTD) is numerically simulated in this study using particle traces. The profiles show similar trends when compared to experimentally observed RTD data. Experimental validation of extruder characteristics and typical temperature profiles in the screw channel for the flow of a very viscous fluid shows good agreement and lends support to the model.

Acknowledgements—This work was supported by the Center for Advanced Food Technology, a New Jersey Commission on Science and Technology Center at Rutgers University. The authors would like to thank Professors V. Sernas and T. H. Kwon and Dr M. Esseghir for discussions throughout this work.

REFERENCES

1. J. D. Dziezak, Single and twin-screw extruders in food processing, *Food Technol.* **43**, 164–174 (1989).

2. Z. Tadmor and C. Gogos, *Principles of Polymer Processing*. Wiley, New York (1979).
3. R. T. Fenner, *Principles of Polymer Processing*. Chemical, New York (1979).
4. Z. Tadmor and I. Klein, *Engineering Principles of Plasticating Extrusion*. Kleiger, Huntington (1978).
5. R. M. Griffith, Fully developed flow in screw extruders, *I & E C Fundam.* **1**(3), 181–187 (1962).
6. H. J. Zamodits and J. R. A. Pearson, Flow of polymer melts in extruders, Part I. Effect of transverse temperature and of a superimposed steady temperature profile, *Trans. Soc. Rheol.* **13**(3), 357–385 (1969).
7. C. Rauwendaal, Throughput–pressure relationship for power-law fluids in single screw extruder, *SPE Tech. Paper* **31**, 30–33 (1985).
8. H. Lappe and H. Potente, Investigations into the throughput behavior of conventional single screw machines, *SPE Tech. Paper* **29**, 174–177 (1983).
9. G. Lidor and Z. Tadmor, Theoretical analysis of residence time distribution functions and strain distribution functions in plasticating screw extruders, *Polym. Engng Sci.* **16**, 450–462 (1976).
10. D. M. Bigg and S. Middleman, Mixing in a screw extruder, model for residence time distribution and strain, *I & E C Fundam.* **13**, 66–71 (1984).
11. R. T. Fenner, The design of large hot melt extruders. Engineering design of plastics processing machinery, University of Bradford, England (1974).
12. R. T. Fenner, Developments in the analysis of steady screw extrusion of polymers, *Polymer* **18**, 617–635 (1977).
13. B. Elbirli and J. T. Lindt, A note on the numerical treatment of the thermally developing flow in screw extruders, *Polym. Engng Sci.* **24**(7), 482–487 (1984).
14. E. E. Agur and J. Vlachopoulos, Numerical simulation of a single-screw plasticating extruder, *Polym. Engng Sci.* **22**(17), 1084–1094 (1982).
15. M. V. Karwe and Y. Jaluria, Numerical simulation of fluid flow and heat transfer in a single screw extruder for non-Newtonian fluids, *Numer. Heat Transfer, Part A* **17**, 167–190 (1990).
16. S. Bruin, D. J. Van Zuilichem and W. Stolp, A review of fundamental and engineering aspects of extrusion of biopolymers in a single screw extruder, *J. Fd Process Engng* **2**, 1–37 (1978).
17. J. Harper, *Food Extrusion*. CRC Press, New York (1980).
18. I. O. Mohamed and R. G. Morgan, Average heat transfer coefficients in single screw extruders of non-Newtonian food materials, Fundamentals of Food Extrusion and Forming Symp., A.I.Ch.E. Summer National Meeting, Boston, Massachusetts (1988).
19. W. A. Atwell, L. F. Hood, D. R. Lineback, E. Varriano-Marston and H. F. Zobel, The terminology and methodology associated with basic starch phenomena, *Cereal Foods World* **33**(3), 306–311 (1988).
20. H. Schlichting, *Boundary Layer Theory*. McGraw-Hill, New York (1979).
21. W. M. Kays and M. E. Crawford, *Convective Heat and Mass Transfer*, 2nd Edn. McGraw-Hill, New York (1980).
22. T. H. Kwon, S. F. Shen and K. K. Wang, Pressure drop of polymeric melts in conical converging flow: experiments and predictions, *Polym. Engng Sci.* **26**(3), 214–224 (1986).
23. Y. Jaluria and K. E. Torrance, *Computational Heat Transfer*. Hemisphere, New York (1986).
24. J. L. Kokini, Physical forces in food systems, Research Accomplishments Report, The Center for Advanced Food Technology, Rutgers University (1988).
25. J. L. Kokini, C. L. Chang, Y. Jaluria, M. V. Karwe, T. H. Kwon, L. S. Lai and V. Sernas, Simulation of transport phenomena in co-rotating twin-screw extruders for starch systems, Second Int. Symp. on Twin-screw Extruder for Food Industry, Japan (1988).
26. S. S. Wang, Private communication, Rutgers University (1990).
27. S. S. Wang, C. C. Chiang, A. I. Yeh, B. Zhao and I. H. Kim, Kinetics of phase transition of waxy corn starch at extrusion temperatures and moisture contents, *J. Fd Sci.* **54**, 1298–1301 (1989).
28. Y. Jaluria, *Computer Methods for Engineering*. Prentice-Hall, Englewood Cliffs, New Jersey (1988).
29. M. Esseghir and V. Sernas, Heat transfer experiments in a single-screw extruder, Int. Symp. Manufacturing and Materials Processing, Dubrovnik, Yugoslavia (1990).

TRANSFERT DE CHALEUR ET DE MASSE DANS UNE VIS D'EXTRUSION POUR DES MATERIAUX NON NEWTONIENS

Résumé—On considère la simulation numérique des mécanismes de transport dans une vis d'extrusion des fluides non Newtoniens tels que les plastiques et les aliments. L'étude simule les transferts de chaleur et de masse dans le canal de la vis, pour un fluide à loi-puissance. L'humidité est prise en compte. Les calculs aux différences finies traitent le système d'équations aux dérivées partielles pour les champs de vitesse, de température et d'humidité, dans un large domaine des paramètres. On tient compte de la variation de la viscosité avec la température et l'humidité. En application de cette analyse, on incorpore la nature réactive des constituants du produit en incluant la vitesse de réaction (gélatinisation) entre l'humidité et le produit. Les contours d'humidité montrent que la gélatinisation se produit d'abord à la base de l'hélice. Une validation expérimentale de quelques résultats numériques a été conduite et les comparaisons sont assez satisfaisantes. On présente des résultats pour la distribution des temps de résidence (RTD), un paramètre important dans l'extrusion. A travers le transfert d'humidité, l'approche présentée peut être étendue facilement aux réactions et au transfert de masse d'autres espèces dans les polymères et d'autres matériaux non Newtoniens.

WÄRME- UND STOFFÜBERGANG IN EINEM EINSCHRAUBENEXTRUDER FÜR NICHT-NEWTON'SCHE MATERIALIEN

Zusammenfassung—Die Transportvorgänge in einem Einschraubenextruder für nicht-Newton'sche Fluide wie Plastik und Lebensmittel werden numerisch untersucht. Die Untersuchung richtet sich hauptsächlich auf die Simulation des Wärme- und Stoffübergangs in einem Schraubenkanal für ein "Power-law"-Fluid. Der Stofftransport von Feuchtigkeit wird betrachtet, da er bei der Nahrungsmittelverarbeitung von besonderem Interesse ist. Der Satz der grundlegenden partiellen Differentialgleichungen für Geschwindigkeit, Temperatur und Feuchtigkeit wird mit Hilfe eines Finite-Differenzen-Verfahrens in einem weiten Parameterbereich gelöst. Dabei wird die Abhängigkeit der Viskosität von Temperatur und Feuchtigkeit berücksichtigt. Das grundlegende physikalische Vorgehen bei der Modellierung der komplizierten Vorgänge des Wärme- und Stofftransports bei nicht elastischen nicht-Newton'schen Materialien wird gezeigt. Die Reaktionsfreudigkeit der Nahrungsmittelbestandteile wird als Anwendung dieser Untersuchungen für Nahrungsmittelsysteme auf Stärkebasis durch die Bestimmung des Reaktionsgrades zwischen Feuchtigkeit und Nahrungsmittel (Gelierung) ermittelt. Als Ergebnisse werden Kurvenverläufe für Geschwindigkeit, Temperatur und Feuchtigkeitskonzentration angegeben. Bei typischen Betriebsbedingungen tritt eine starke viskose Dissipation auf. Die Feuchteverteilung zeigt, daß die Gelierung von Stärke typischerweise zuerst am Schraubenfuß auftritt. Der Einfluß unterschiedlicher Parameter auf den Druckaufbau im Extruderkanal wird bestimmt und auf der Grandlage der physikalischen Vorgänge diskutiert. Einige der numerischen Ergebnisse werden experimentell bestätigt—die Übereinstimmung ist recht gut. Zusätzlich werden Ergebnisse für die Verweilzeitverteilung vorgestellt, die einen wichtigen Auslegungsparameter bei der Extrusion darstellt. Obwohl diese Untersuchung sich mit dem Feuchtigkeitstransport beschäftigt, kann die grundlegende Vorgehensweise leicht auf Reaktion und Stoffübergang anderer Stoffe in polymeren und anderen nicht-Newton'schen Materialen ausgedehnt werden.

ТЕПЛО- И МАССОПЕРЕНОС В ОДНОВИНТОВОМ ЭКСТРУДЕРЕ ДЛЯ НЕНЬЮТОНОВСКИХ МАТЕРИАЛОВ

Аннотация—Численно моделируются процессы переноса в одновинтовом экструдере, применяемом для таких неньютоновских жидкостей как пластмассы и пищевые продукты. Целью исследования является моделирование тепло- и массопереноса при течении степенной жидкости в винтовом канале. В качестве среды, где происходит массоперенос, рассматривается влага, поскольку она представляет особенный интерес при переработке пищевых продуктов. Методом конечных разностей решается определяющая система уравнений в частных производных, описывающих поля скоростей, температур и влагосодержания в широком диапазоне определяющих параметров. Учитывается изменение вязкости с изменением температуры и влагосодержания. Описан основной физический метод моделирования взаимосвязанных процессов тепло- и массопереноса в случае неупругих неньютоновских материалов. Применение предложенного анализа к системам пищевых продуктов на основе крахмала иллюстрируется на примере учета химической активности компонентов пищевых продуктов, а именно, скорости реакции (желатинирования) между вгагой и продуктом. Полученные результаты представлены в виде кривых скорости, температуры и влагосодержания. Найдено, что при типичных режимных параметрах возникают сильные эффекты вязкостной диссипации. Кривые влагосодержания свидетельствуют о том, что желатинирование крахмала, как правило, происходит сначала у основания винта. Определяется и обсуждается в рамках исследуемого процесса влияние различных определяющих параметров на новышение давления в канале экструдера. Получено удовлетворительное согласие между некоторыми численными результатами и экспериментальными данными. Представлены также результаты распределения времени пребывания, являющегося важным параметром расчета экструдера. Несмотря на то, что в данной работе исследуется влагоперенос, предложенный метод может быть легко обобщен на реакции и массоперенос других веществ в полимерах и в других неньютоновских материалах.